Opportunities and Challenges for Long-Distance Transmission in Hollow-Core Fibres

This article has been accepted for publication in IEEE/OSA Journal of Lightwave Technology. This is the author's version which has not been fully edited and content may change prior to final publication. Citation information: DOI 10.1109/JLT.2021.3140114

Opportunities and Challenges for Long-Distance Transmission in Hollow-Core Fibres

Pierluigi Poggiolini, Francesco Poletti

***Abstract*—Anti-resonant hollow-core fiber of the Nested Antiresonant Nodeless type (NANF) has been showing a steady decrease in loss over the last few years, gradually approaching that of standard Single-Mode Fiber (SMF). It already by far outperforms SMF as to non-linear effects, which are three to four orders of magnitude lower in NANF than in SMF. Theoretical predictions and experimental evidence also hint at a much wider usable bandwidth than SMF, potentially amounting to several tens of THz. Propagation speed is 50% faster, a key feature in certain contexts.**

In this paper we investigate the potential impact of possible future high-performance NANF on long-haul optical communication systems, assuming NANF continues on its current steady path towards better performance. We look at the system throughput in different long-haul scenarios, addressing links of various length, from 100 km to 4,000 km, and different NANF optical bandwidths, loss and total launch power. We compare such throughput with a benchmark state-of-the-art SMF Raman-amplified C+L system. We found that NANF might enable relative throughput gains vs. the benchmark on the order of 1.5x to 5x, at reasonable NANF and system parameter values.

We also study the problem of the impact of NANF Inter-Modal-Interference (IMI) on system performance and show that a value of -60 dB/km, close to the currently best reported values, is low enough to have no substantial harmful effect.

We finally look at a more long-term scenario in which NANF loss gets below that of SMF and we show that in this context repeaterless or even completely amplifierless systems might be possible, delivering 300-400 Tb/s per NANF, over 200 to 300 km distances. The system simplification and ease of wideband exploitation implied by these systems might prove quite attractive especially in densely populated regions where inter-node distances are modest.

While several technological hurdles remain before NANF-based systems can be practical contenders, in our opinion NANF appears to have the potential to become an attractive and possibly disruptive alternative to conventional solid-core silica fibers.

***Index Terms*—hollow-core fibers, anti-resonant hollow-core fibers, nested anti-resonant nodeless fibers, NANF, WDM, optical networks, coherent systems, long-haul transmission**

I. Introduction

CAPACITY demand growth projections have been showing for some time that substantial throughput saturation would be felt in increasingly wider segments of the optical transport networks, around the beginning of the 2020s. This seems to be happening as predicted [1].

Pierluigi Poggiolini is with Politecnico di Torino, 10129, Torino, Italy, e-mail: pierluigi.poggiolini@polito.it

Francesco Poletti is with the Optoelectronics Research Center, University of Southampton, United Kingdom

This study was supported by the European Research Council (ERC, grant agreement n 682724), by Lumenisity Ltd., by the PhotoNext Center of Politecnico di Torino and by the CISCO SRA contract OptSys 2022.

Manuscript received August 1st, 2021.

In anticipation of this event, several countermeasures have been explored. Among the proposed solutions, some leverage increased transponder DSP complexity, such as better codes and more sophisticated modulation schemes, as well as non-linearity mitigation algorithms of various form. Others target the use of non-conventional transmission bands (L, O, S, E, etc.) to increase the overall per-fiber WDM bandwidth. Yet others focus on Space Division Multiplexing (SDM), which aims at increasing the number of independent orthogonal 'channels' (in the information-theory sense) available for transmission. This is achieved by either building fibers that carry multiple orthogonal modes in their core (Few Mode Fibers, FMFs [2]) or fibers with several single-mode cores (Multi-Core Fibers, MCFs [3]), or combinations thereof.

Among all of the above-mentioned techniques, transponder-based ones are currently dominating the scene, with wide deployment of sophisticated DSP in commercial products. On the other hand, further efforts in this direction are expected to yield limited and diminishing returns [1]. As for the use of non-conventional bands, L-band is now commercially available. However, further extensions towards other bands appear more difficult and incrementally less effective, at least within the long-haul scenarios addressed in this paper [4].

If installing entirely new cables becomes inevitable, MCF currently appears as the technology which is the closest to practical exploitability. Nonetheless, the techno-economical advantage of the deployment of MCF vs. the installation of multiple conventional single-mode fibers (SMFs) is still being debated. Substantial uncertainty in this respect also comes from the need to develop the whole range of components and subsystems needed for MCFs-based networks at an economically viable cost.

In this still uncertain landscape, an alternative technology, *Hollow-Core Fibers* (HCFs), has emerged as a further possible contender. HCFs are not new: they have been studied for over two decades [5]. Theoretically they would offer several important advantages. Among them: ultra-low non-linearity (3 to 4 orders of magnitude lower than SMF); 50% faster light propagation speed than in SMF, which is critical in certain applications; low dispersion; even more important, some structures potentially have *an exploitable bandwidth which may be substantially greater than that of SMF* and unhindered by the problem of Inter-channel Stimulated Raman Scattering (ISRS).

Unfortunately, for a long time low-loss proved very difficult to achieve in HCFs, remaining well above the dB/km mark. At the same time, Inter-Modal-Interference (IMI) has also been a problem in HCFs, as these fibers are intrinsically

This article has been accepted for publication in IEEE/OSA Journal of Lightwave Technology. This is the author's version which has not been fully edited and content may change prior to final publication. Citation information: DOI 10.1109/JLT.2021.3140114

multimodal. In 2014, however, a new type of HCFs called Nested Antiresonant Nodeless Fibers (NANFs) was proposed, having the potential to address both loss and IMI problems simultaneously [6].

Specifically, the addition of nested tubes would reduce dramatically the loss from non-nested tubular designs [7], while the absence of contact points or nodes between the cylindrical tubes (present, for example in the nested concept proposed in [8]) would eliminate spectral resonances and widen the low-loss window, while also reducing leakage loss by a factor of approximately 10. The loss of such NANFs has been quickly lowered from initial very high values down to 1.3 dB/km in 2018 [9], 0.65 dB/km in 2019 [10], 0.28 dB/km in 2020 [11] and remarkably 0.22 dB/km in 2021. In fact, the theoretical minimum loss of NANFs, assuming perfect fabrication with no imperfection, is lower than that of SMF [6] (see also Sect. II). Whether lower than SMF loss is actually attainable in a practical NANF, it is still an open question, but progress in loss reduction so far has been steady.

As for IMI, it occurs because, as mentioned, NANFs are intrinsically multimodal. Although they can achieve an effective single-mode operation by inducing a large loss to all higher-order modes, IMI can still be significant if the higher-mode suppression mechanism is not strong enough. In a transmission experiment over NANF carried out in 2020, IMI was found to be the main limiting factor, with an estimated value of -35 dB/km [13]. However, through improvements in fiber design, in a more recent record transmission experiment, IMI has been reduced to between -45 and -55 dB/km [14]. This has been possible thanks to a judicious choice of tube number and size that granted higher loss for the higher-order modes.

Thanks to both loss and IMI improvements, DWDM long-haul experiments over NANF have shown very quick progress, with WDM PM-QPSK transmission at 32 GBaud reaching 341 km [12], 618 km [13] and more than 4,000 km [14], over the course of just the last three years. Note that these experiments were performed on recirculating loops, where the NANF section had length of 4.8, 7.7 and 11.5 km, respectively.

Also, confirming early predictions [6], various recent measurements have shown that NANFs can have a bandwidth which may be much larger than SMF, *in the realm of tens of THz* [10], i.e., several times the C+L bandwidth (see Sect. II). This is quite significant since, ultimately, it is bandwidth that would truly make NANFs a strong contender in the quest for a solution to the problem of SMF bandwidth exhaustion.

While individual NANFs reported to date have already shown one or two features out of: low loss, low IMI and wide bandwidth, at present no NANF has yet achieved all three together. In this paper we assume that progress will be made towards improving all three aspects together. Then, we try to assess the relative merit of using NANFs vs. SMFs as a function of such progress. We perform the analysis over a few typical system scenarios, with diversified assumptions. In the end, we try to address key questions related to the potential of NANFs to achieve a substantially larger throughput performance as compared to SMF-based systems and we discuss its possible implications.

This paper is structured as follows. In Sect. II, an introduction to NANF and its main potential advantages is provided. In Sect. III the theory and analytical tools used to perform the system investigation are laid out. In Sect. IV the scenarios of interest are described and a comparison between SMF and NANF is carried out in detail for each of them. Sect. V is devoted to analyzing the possibility of performing transmission in NANF over regional distances without resorting to optical amplifiers. A discussion section is next, Sect. VI, where NANF vs. SMF are compared in a more encompassing fashion over a wide range of system lengths, from 100 to 4,000 km, and under different system parameter assumptions. Conclusions follow.

This paper is a follow-up submission to the OFC 2021 invited paper [15].

II. The Nested Antiresonant Nodeless Fiber

NANFs are formed by sets of non-touching nested glass tubes that surround a gas-filled central core [6]. The tube thickness is chosen to be similar for all tubes, and such that at the wavelength of interest the fiber operates in antiresonance, where light-glass overlap can be minimized. The absence of glass nodes (all tubes are only attached to an outer jacket tube) guarantees a transmission window spanning over one octave free of undesired resonances, while through the choice of adequate structural dimensions one can obtain a low rate of light leakage for the fundamental mode and a simultaneously high leakage for all other core-guided modes, hence, potentially very low IMI.

One of the most attractive features of these fibers for the purpose of data transmission is their *intrinsically low nonlinearity*. Although this has not yet been measured accurately for state-of-the-art NANFs, by combining the small glass overlap (which can be as small as 0.003%) with the Kerr nonlinearity of typical gases ($\sim$ 3 orders of magnitude lower than silica), and taking into account the larger effective area of NANFs (with a mode field diameter, MFD, of 22-25 μm vs 10-12 μm of glass-guiding fibers), nonlinear coefficients on the order of $\gamma = 10^{-4}$ to 10^{-3} (W km)$^{-1}$ are predicted. In later sections of this paper we will estimate the advantages that this brings to different application scenarios.

As one would expect for fibers guiding predominantly in air, the chromatic dispersion of NANFs is also small in magnitude and spectrally flat. It can be shown that in the fiber low loss spectral region dispersion can be approximated quite accurately by that of a simple circular tube [16], for which $D = k(\lambda/R^2)$, where k is a numerical constant, λ the operational wavelength and R the core radius. For fibers operating in the C-band with core diameters of 30-35 μm, D is in the range of 2.5-3.5 ps/(nm·km), and dispersion slope is $\sim$10 times smaller than for step index solid core fibers.

In addition, state-of-the-art NANFs present 30% lower latency than glass guiding fibers [17], a negligible back-scattering coefficient (measured to be 45 dB below that of glass guiding fibers [18]), and they are unlikely to suffer from phase noise induced by guided acoustic wave Brillouin scattering (GAWBS) [19] which can be detrimental in some long distance coherent links. They are also immune from fiber fuse problems for any practical launched power, which enables the launch of

This article has been accepted for publication in IEEE/OSA Journal of Lightwave Technology. This is the author's version which has not been fully edited and content may change prior to final publication. Citation information: DOI 10.1109/JLT.2021.3140114

signals with orders of magnitude higher power than in current systems [20].

Of particular interest for this work is also their capacity to provide, potentially, a broader low loss bandwidth than conventional glass-guiding fibres. In conventional fibers the minimum loss region is dictated by glass-induced loss mechanisms, and occurs at the interception between the Rayleigh scattering curve (proportional to λ^{-4}) and the steep infrared multi-photon absorption curve ($C \cdot e^{-D/\lambda}$) of silica glass [21]. The resulting total loss curve can be seen in Fig. 1(b) for a standard single-mode fiber (SMF, black curves).

In a HCF like the NANF, where light can be guided almost entirely in an air core, the spectral shape of its loss and the resulting bandwidth over which this can be achieved are not determined by fundamental glass mechanisms. Rather, the typical U-shaped loss curve is caused by coupling to glass tube modes at short wavelengths and by leakage loss at long wavelengths, with surface scattering [6] and micro/macro bend phenomena [11] also possibly playing a role in determining the exact shape and bandwidth.

Estimating the value of loss and bandwidth that NANFs or their improved successors (of which many designs have been already theoretically proposed) might one day achieve falls beyond the scope of this paper. Here we will rather adopt a simple scaling rule to illustrate that considerably wider bandwidths than glass-guiding fibers are theoretically possible.

Fig. 1(a) plots the measured loss (up to the 1700 nm limit of the available optical spectrum analyzer, OSA) of a 0.28 dB/km state-of-the-art NANF [11]. The figure also shows the excellent match with the simulated loss curve of the same fiber, obtained by modeling the leakage of its fabricated cross-section and by adding to it a small estimated microbend contribution, with a negligible surface scattering loss [11]. The characteristic U-shape of its loss has a short wavelength edge at 1100 nm determined by coupling with glass tube modes and a long wavelength edge at 2100 nm caused by leakage loss.

In Fig. 1(b) we have made the assumption that through improvements in structure and fabrication process such a loss level can be reduced, but that its spectral shape remains unchanged. Note that even broader bandwidths are theoretically possible through improved designs that reduce the long wavelength leakage. We have also neglected the water vapor absorption (1350-1450 nm) which is not fundamental in origin. For illustration, we plot three curves where the simulated loss curve in Fig. 1(a) has been rigidly down-scaled to a minimum value of 0.145, 0.1 and 0.05 dB/km (curves A, B and C, respectively). A small spectral shift, easily achievable during fabrication with controllable modifications in the tube membrane thickness, was also applied. For comparison, we also plot the loss of a standard germanium doped SMF (black curves).

Curve A shows that if NANF achieved the same minimum C-band loss as current PSCF (0.145 dB/km [22]), the bandwidth offered by the hollow core fiber would be wider. For example, PSCF offer about 180 nm of spectrum with loss below 0.17 dB/km (1450-1630 nm), whereas NANF would offer 230 nm (1450-1680 nm). If the NANF minimum loss could be reduced down to 0.1 dB/km, curve B shows that a

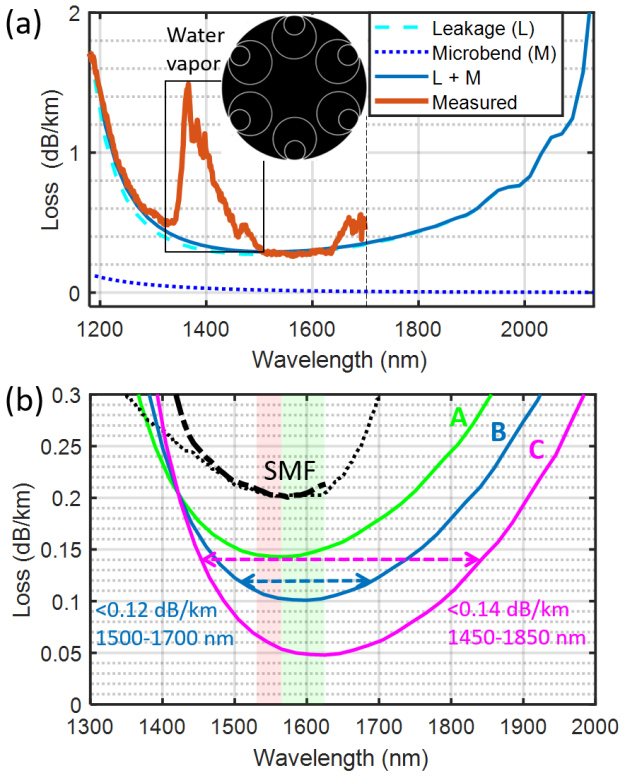

Fig. 1. **(a)** Measured and simulated loss for a 0.28 dB/km NANF, the cross-sectional structure of which is shown in the inset [11]; **(b)** Optical bandwidth prediction of what future NANFs might offer, obtained by rigidly down-scaling and spectrally shifting the simulated curve in **(a)**. Three cases illustrate scenarios where the minimum loss reaches 0.145 dB/km (A), 0.1 dB/km (B) and 0.05 dB/km (C). For comparison, the loss of standard SMF is also shown (black curves).

200 nm bandwidth, from 1500 to 1700 nm would in principle be possible at a loss below 0.12 dB/km. Finally, curve C shows that in a NANF with a minimum loss of 0.05 dB/km, propagation below 0.14 dB/km would be possible over as many as 400 nm, from 1450 to 1850 nm.

Clearly, these are only illustrative examples based on the assumption that loss remains dominated by leakage and that it therefore maintains the same spectral shape as in current fibers. It is however likely that surface scattering might start to play a role down to around 0.1 dB/km loss levels. This would in practice introduce a much flatter wavelength dependence (roughly proportional to λ^{-1} or less) to the overall loss profile shown in Fig. 1(b) [6]. Since the overall spectral dependence is difficult to predict, in the following simulations we will neglect such effect and assume a spectrally flat level of loss. We leave to future work the task to finesse these assumptions and related results.

Finally, possible future NANF-based systems will need to splice NANFs-to-NANFs, as well as conceivably NANFs to solid-core fibers. Splice loss between hollow-core NANFs is currently at the 0.1-0.2 dB level, while the splice loss to solid core single-mode fibers tends to be higher (0.5dB), if mode-field mismatch and Fresnel reflections are not properly managed. With suitable optimization though, SMF-NANF connection loss of only 0.15 dB has been recently demonstrated [23]. These values are only marginally higher than

the typical splicing loss that is achievable with conventional solid core fiber technology, with further potential for additional improvement. Therefore, in the context of this study, we have decided to neglect this aspect, with one exception: the repeaterless/amplifierless scenarios discussed in Sect. V, where splice loss is important.

III. Methodology

The aim of this study was that of assessing the relative merit of using either SMF or NANF in optical transmission systems. We focused on certain system scenarios, which we deemed as sufficiently 'typical' and yet sufficiently diversified to provide an encompassing comparison.

The study was carried out under the following set of general assumptions:

1) transmission is performed with ideal Gaussian-shaped constellations
2) spans are all identical
3) fiber loss and dispersion are frequency-independent within the assumed usable bandwidth
4) loss is exactly compensated for span by span
5) Inter-channel Stimulated Raman Scattering (ISRS) in SMFs is not taken into account

Regarding (5), such assumption essentially favors SMF or, in other words, leads to a *conservative* estimate of the potential advantage of using NANF.

In the following, for the readers' convenience, we provide consistent units for all the quantities that are introduced.

To compare systems using different fibers in possibly quite different configurations, we focused on what is arguably the most significant system performance indicator: the maximum data throughput through the link. If noise at the end of the link was additive, white and Gaussian (AWGN), adapting Shannon's formula, similarly to what was done for instance in [24], [25], the link throughput T (Tb/s) would be:

$$T = 2\frac{R_{\mathrm{ch}}}{\Delta f} B_{\mathrm{WDM}} \log_2\left(1+\mathrm{SNR}\right) \tag{1}$$

where B_{WDM} is the total optical bandwidth used for transmission (THz), Δf is the channel spacing (THz), R_{ch} is the channel symbol rate (TBaud) and SNR is the signal-to-noise ratio observed on the received constellation of each channel.

Under the assumption that a *matched Rx filter* is used and that non-linear interference (NLI) due to the fiber Kerr effect can be considered as additive Gaussian noise approximately white (flat) over each channel, the SNR of an ideally demodulated constellation can be written as:

$$\mathrm{SNR} = \frac{P_{\mathrm{ch}}}{P_{\mathrm{ASE}} + P_{\mathrm{NLI}} + P_{\mathrm{IMI}}} \tag{2}$$

where P_{ch} is the transmitted power per WDM channel, P_{ASE} is the filtered amplified spontaneous emission (ASE) noise power due to the amplifiers, P_{NLI} is the filtered non-linear interference (NLI) noise due to the Kerr effect and P_{IMI} is the disturbance due to IMI (relevant to NANFs only), all in Watts.

When lumped amplification is used, P_{ASE} is given by:

$$P_{\mathrm{ASE}} = N_{\mathrm{span}}\, h\nu F R_{\mathrm{ch}} \cdot (G-1) \tag{3}$$

where h is Planck's constant, ν is the WDM comb center frequency and $(h\nu)$ has units of Joule, F is the amplifiers noise figure (dimensionless), N_{span} and L_{span} are the link number of spans and length of each span (km), and G is the amplifier gain (dimensionless). Under assumption (4) above, then:

$$G = e^{-2\alpha L_{\mathrm{span}}} \tag{4}$$

where 2α is the fiber (power) loss (1/km). Besides lumped amplification, we will also consider mixed lumped/distributed amplification. We will do it by using an *effective* noise figure, as discussed later.

The term P_{NLI} is computed using the closed-form GN-model approximation Eq. (15) in [26]. Accordingly, we can write:

$$P_{\mathrm{NLI}} = \left(\eta \cdot P_{\mathrm{ch}}^3\right) \ , \tag{5}$$

$$\eta = N_{\mathrm{span}} \frac{4\gamma^2}{27\pi\left|\beta_2\right|\alpha R_{\mathrm{ch}}^2} \mathrm{asinh}\left(\frac{\pi^2\left|\beta_2\right|}{4\alpha} R_{\mathrm{ch}}^2 N_{\mathrm{ch}}^{2\frac{R_{\mathrm{ch}}}{\Delta f}}\right) \tag{6}$$

where N_{ch} is the number of WDM channels in the comb, β_2 and γ are fiber dispersion (ps^2/km) and non-linearity coefficient 1/(W·km), respectively. Eqs. (5)-(6) provide P_{NLI} for the center channel in the comb. For simplicity, we assume that the same P_{NLI} affects each WDM channel.

The term P_{IMI} is modelled similar to what was done for instance in [25] for inter-core crosstalk:

$$P_{\mathrm{IMI}} = \kappa P_{\mathrm{ch}} L_{\mathrm{tot}} \tag{7}$$

where $L_{\mathrm{tot}} = N_{\mathrm{span}} \cdot L_{\mathrm{span}}$ is the total link length (km) and κ is the IMI strength (1/km).

From Eqs. (2)-(7), the optimum launch power $P_{\mathrm{ch}}^{\mathrm{opt}}$ and the corresponding maximum signal-to-noise ratio $\mathrm{SNR}_{\mathrm{MAX}}$ can be found in closed-form:

$$P_{\mathrm{ch}}^{\mathrm{opt}} = \sqrt[3]{\frac{P_{\mathrm{ASE}}}{2\eta}} \quad , \quad \mathrm{SNR}_{\mathrm{MAX}} = \frac{P_{\mathrm{ch}}^{\mathrm{opt}}}{\frac{3}{2}P_{\mathrm{ASE}} + \kappa L_{\mathrm{tot}}} \tag{8}$$

Interestingly, as also noted in [25], $P_{\mathrm{ch}}^{\mathrm{opt}}$ does not depend on κ (the strength of IMI).

Substituting $\mathrm{SNR}_{\mathrm{MAX}}$ into Eq. (1) yields the maximum link throughput T_{MAX}. In their simplicity, Eqs. (1)-(8) represent a powerful tool which we will use to discuss quite diverse link scenarios. The assumptions and approximations underlying these formulas have been discussed in prior literature, such as [27], [28], but given that we will use them in a rather unconventional scenario, we will also show results of *specific split-step simulative validations*.

IV. Scenarios

In this section we look at different scenarios, where we compare NANF vs. SMF, in terms of throughput.

All the tested scenarios assume transmitting Gaussian-modulated channels at R_{ch}= 64 GBaud with spacing Δf= 87.5 GHz and roll-off 0.1 . A 3 dB back-to-back SNR penalty vs. ideal Eq. (1) is assumed as well.

For the NANF, we assume a NL coefficient γ= $5{\cdot}10^{-4}$ (W km)$^{-1}$. We also assume a somewhat lower dispersion value D= 2 ps/(nm km) than predicted by design simulations. This

This article has been accepted for publication in IEEE/OSA Journal of Lightwave Technology. This is the author's version which has not been fully edited and content may change prior to final publication. Citation information: DOI 10.1109/JLT.2021.3140114

causes P_{NLI} to be somewhat overestimated, leading to conservative throughput estimates with NANF. We then sweep the NANF attenuation over the range 0.5 dB/km to 0.05 dB/km, which are values ranging between currently reported values and values that might ideally be possible with future NANFs ([6], see also Sect. II and Fig. 1). As a benchmark, we use SMF, with loss 0.2 dB/km, dispersion D= 16.7 ps/(nm km) and non-linearity coefficient γ= 1.3 (W km)$^{-1}$.

A. Scenario #1: C+L band, 1000 km

The first scenario we consider is a long-haul terrestrial link consisting of 10 spans of 100 km each. For both SMF and NANF we assume C+L WDM bandwidth transmission (about 9 THz), corresponding to 103 channels. This means that in this first scenario we do not take advantage of NANF's potentially larger bandwidth. We also assume a favorable amplification solution for SMF, whereby hybrid Raman/EDFA is used, with backward Raman pumping, at an overall *effective* noise figure F= 0 dB. For NANF we assume instead lumped amplification, with F= 5 dB, since Raman is not possible due to the extremely low NANF nonlinearity.

In these conditions, the maximum throughput delivered by SMF, $T_{\mathrm{MAX}}^{\mathrm{SMF}}$, as found through Eqs. (1)–(8), is 71.4 Tb/s, at an optimum total launch power of 20.2 dBm. Note though that the actual power into SMF is much higher (in the backward direction) because of the Raman pumps, possibly between 1 and 2 Watts. Note also that this value of max throughput is obtained at a rather high net spectral efficiency of 10.8 bits/symb (5.4 net per polarization), a critical aspect that we will come back to later.

Fig. 2(a) is a contour plot of the ratio ρ between the throughput that can be obtained using the NANF, calculated using Eqs. (1)–(8), vs. $T_{\mathrm{MAX}}^{\mathrm{SMF}}$, that is:

$$\rho = T^{\mathrm{NANF}} / T_{\mathrm{MAX}}^{\mathrm{SMF}} \tag{9}$$

The horizontal and vertical axes represent NANF loss in dB/km and launch power in dBm. The thick red line marks the points where the NANF throughput is equal to the SMF maximum throughput, that is where $T^{\mathrm{NANF}} = T_{\mathrm{MAX}}^{\mathrm{SMF}}$. The thin dashed line marks the points that are optimum for NANF throughput maximization. This optimum is induced by Kerr non-linearity which, albeit extremely small in NANF, does show up at ultra-high launch powers.

Such launch powers are unrealistic, but we kept them in Fig. 2(a), and following plots, precisely to show that non-linearity becomes a limiting factor at launch powers that are beyond the realm of practical values. Only if one assumes that NANF loss is substantially lower than SMF, then the optimum launch power line comes down to less unrealistic values (40 or even 35 dBm in Fig. 2(a), for loss below 0.1 dB/km). However, as we shall comment later on, these operating points are likely impractical for other reasons.

The star markers represent points that have been validated by full (C+L)-band split-step simulations based on the Manakov equation. Validation was performed by comparing the NANF center WDM channel mutual information measured on

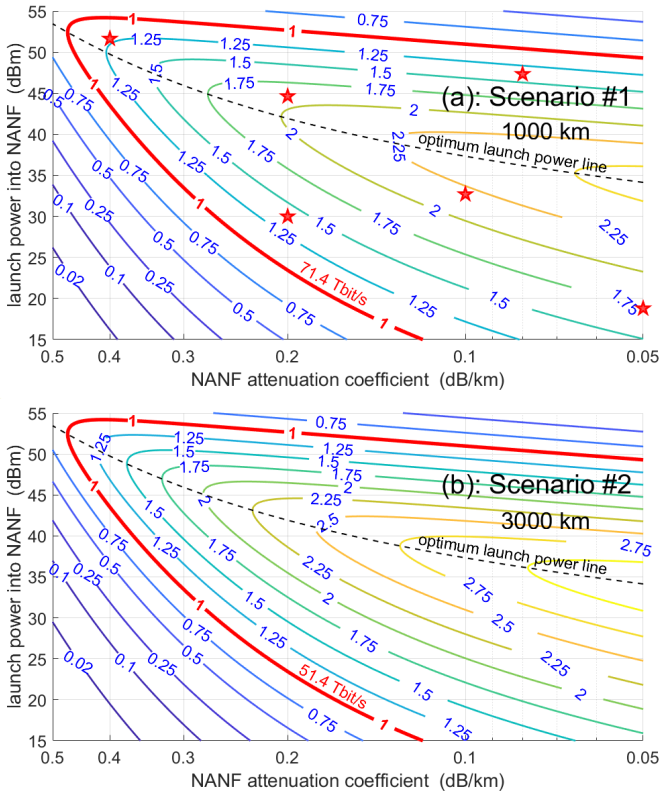

Fig. 2. Isolines showing the ratio ρ of NANF system throughput vs. the SMF maximum system throughput (71.4 Tb/s), over the plane (NANF loss, NANF launch power). All links operate over the C+L band (9 THz). The red isoline marks the ratio 1, i.e., same NANF throughput as maximum SMF throughput. Star markers are values verified through full-band split-step simulations. IMI is assumed to be absent or negligible. **(a):** Scenario #1, 1000 km (10 spans of 100 km). **(b):** Scenario #2, 3000 km (30 spans of 100 km).

the split-step simulation, $\mathrm{MI}_{\mathrm{SIM}}^{\mathrm{NANF}}$, with the one predicted by Shannon's formula as:

$$\mathrm{MI}^{\mathrm{NANF}} = 2 \cdot \log_2 (1 + \mathrm{SNR}),$$

where SNR is given by Eq. (2). We found the mean MI error to be 1.4%, while the max error was 2.6%. We consider these results as sufficient evidence of the reliability of the analytical approach, within the mentioned assumptions.

Interestingly, a greater NANF throughput than SMF can be seen in Fig. 2(a) even at values of NANF loss greater than the loss of SMF. For instance, for a NANF loss of 0.275 dB/km, a throughput 25% greater than SMF is ideally possible, for 35 dBm launch power. If same launch power is imposed, a 50% greater than SMF throughput is found for 0.235 dB/km loss. If instead we assume same loss for the NANF as for SMF (0.2 dB/km), then a 50% greater throughput than SMF can be reached at a lower launch power of 31.8 dBm, still large but comparable to the power of the Raman pumps into the SMF.

These appear as favorable results for NANF, but it must be pointed out that achieving such higher values of throughput than SMF implies transmission at an increased number of bits/symbol per channel $\mathrm{Ch}_{\mathrm{b/s}}$, which can be written as:

$$\mathrm{Ch}_{\mathrm{b/s}} = \frac{T\,\Delta f}{B_{\mathrm{WDM}} R_{\mathrm{ch}}} \tag{10}$$

This article has been accepted for publication in IEEE/OSA Journal of Lightwave Technology. This is the author's version which has not been fully edited and content may change prior to final publication. Citation information: DOI 10.1109/JLT.2021.3140114

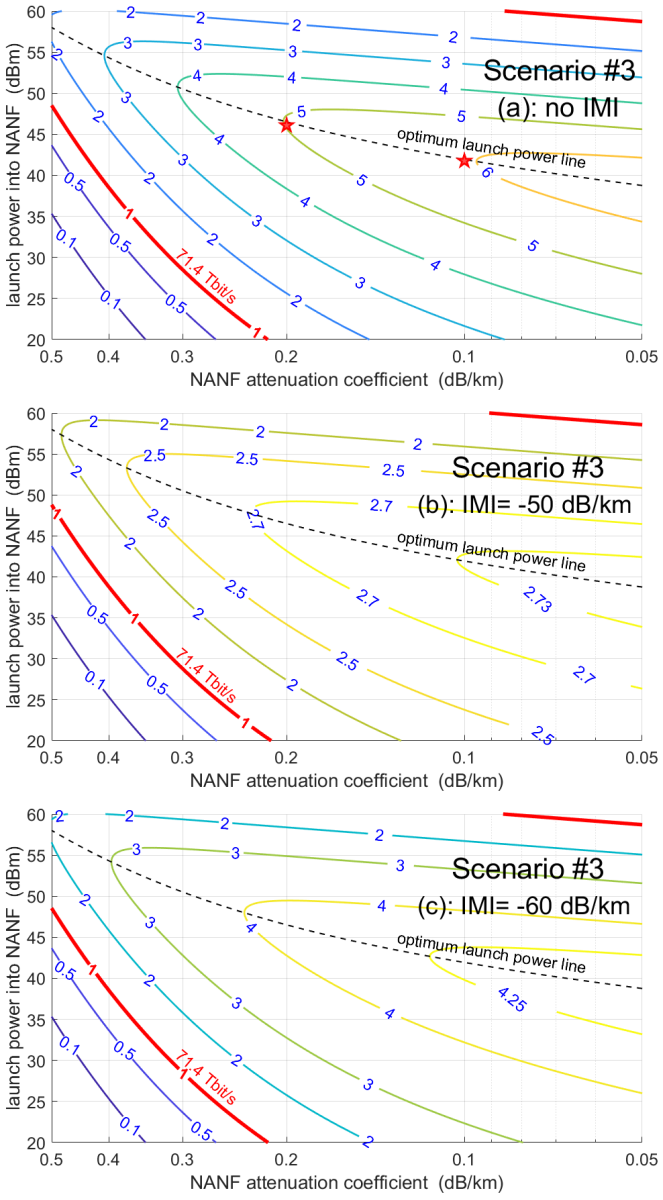

Fig. 3. Scenario #3. Isolines showing the ratio ρ of NANF system throughput vs. the SMF maximum system throughput (71.4 Tb/s), over the plane (NANF loss, NANF launch power). The test link is 1000 km long (10 spans of 100 km each). The NANF systems operate over the 1500-1700 nm band (23.5 THz), the benchmark SMF system over the C+L bands (9 THz). The red isoline marks the ratio 1, i.e., same NANF throughput as maximum SMF throughput. Star markers are values verified through full-band split-step simulations. **(a):** no IMI. **(b):** IMI -50 dB/km. **(c):** IMI -60 dB/km.

In this first scenario the same C+L optical bandwidth B_{WDM} is considered for both SMF and NANF and therefore when $T^{\mathrm{NANF}} > T^{\mathrm{SMF}}$, then Eq. (10) implies that $\mathrm{Ch}_{\mathrm{b/s}}^{\mathrm{NANF}} > \mathrm{Ch}_{\mathrm{b/s}}^{\mathrm{SMF}}$, proportionally. But, as previously mentioned, the value of $\mathrm{Ch}_{\mathrm{b/s}}$ at max throughput for SMF is already rather high: $\mathrm{Ch}_{\mathrm{b/s}}^{\mathrm{SMF}}$ =10.8 bits/symb. To achieve a higher throughput with NANF, $\mathrm{Ch}_{\mathrm{b/s}}^{\mathrm{NANF}}$ then needs to be even higher.

As an example, to attain a 50% throughput increase on NANF, $\mathrm{Ch}_{\mathrm{b/s}}^{\mathrm{NANF}} = 16.2$ (net) bits/symb transmission (8.1 net per polarization) is necessary. This would likely require using constellations as large as 1024-QAM, a rather challenging proposition. While wireless and ADSL commercially use constellations of several thousand symbols, it is an open question whether this is practically achievable in optical communications.

Interestingly, the problem of high $\mathrm{Ch}_{\mathrm{b/s}}$ gets alleviated when going to longer transmission distances (see Scenario #2 immediately following). It is also alleviated when a larger NANF bandwidth is assumed (see Scenario #3 later).

B. Scenario #2: C+L band, 3000 km

This scenario assumes the exact same parameters as the previous one, with the only difference of link length being now 3000 km (30 spans of 100 km each) rather than 1000 km.

The results are shown in Fig. 2(b). The plot is quite similar to Fig. 2(a), but in general a slight improvement of ρ can be observed. For instance, at loss 0.2 dB/km and 31.8 dBm launch power, NANF delivers 1.7x over 3000 km, whereas it delivered 1.5x over 1000 km. This increase, when distance is increased, can be shown to be due to the analytical form of Eq. (1) and, specifically, how operating at the lower system SNRs, which are found at longer distances, affects it.

Quite significantly from a practical viewpoint, the problem of extreme values of $\mathrm{Ch}_{\mathrm{b/s}}$ gets alleviated in Scenario #2. The values of both T^{NANF} or T^{SMF} are now lower, because the 3000 km link operates at lower SNRs than the 1000 km one. Specifically, with reference to Eq. (10), $T_{\mathrm{MAX}}^{\mathrm{SMF}}$ is now 51.4 Tb/s, resulting in $\mathrm{Ch}_{\mathrm{b/s}}^{\mathrm{SMF}}$ = 7.8 bits/symb. Consequently, a 1.5x throughput increase for NANF now requires $\mathrm{Ch}_{\mathrm{b/s}}^{\mathrm{NANF}} = 11.7$ bits/symb, certainly challenging but likely feasible, at least in prospect. Of course, when looking at even higher multiples, ideally possible at substantially lower loss than SMF, the resulting needed $\mathrm{Ch}_{\mathrm{b/s}}$ values still appear prohibitively large.

C. Scenario #3: 1500-1700 nm, 1000 km

In this third scenario we assume that the NANF usable bandwidth now extends from 1500 to 1700 nm, or about 23.5 THz (269 WDM channels). We look at 1000 km, 10 spans of 100 km each. For the NANF we assume that lumped amplification is available with an average F= 7 dB, a 2-dB degraded noise figure from scenario #1, to account for a possibly inferior performance of the non-EDFA amplifiers needed to cover the S and U bands. Specifically, while S-band lumped amplifiers are commercially available, U-band is still somewhat of an open problem. Note though that solutions for the U-band might also come in the form of lumped Raman amplifiers, in case doped-fiber solutions proved less viable.

As benchmark, we still use SMF over the C+L band, with hybrid Raman/EDFA at a noise figure F= 0 dB, for a maximum throughput of $T_{\mathrm{MAX}}^{\mathrm{SMF}}$=71.4 Tb/s. The reason why we keep as benchmark C+L band SMF is because extending transmission over the 1500-1700 nm band in SMF, while it appears possible, does not seem to be easily capable of yielding substantial overall throughput increase especially in long-haul systems, due to various circumstances: higher loss in the U band; extremely strong inter-channel stimulated Raman

This article has been accepted for publication in IEEE/OSA Journal of Lightwave Technology. This is the author's version which has not been fully edited and content may change prior to final publication. Citation information: DOI 10.1109/JLT.2021.3140114

scattering (ISRS); the fact that SMF would no longer be able to enjoy full Raman amplification over such a broad band, leading to a quite significant deterioration of noise figure. For these reasons, we deem SMF over C+L with Raman as a 'sweet spot' that constitutes a significant benchmark for any new technology, including possibly extending optical bandwidth in SMF itself.

The NANF results for this new scenario are shown in Fig. 3a. Note that two points on the plot were verified through full-band split-step simulations, both returning an MI less than 2% away from the prediction of Eqs. (1)-(5).

Clearly, much more favorable multiples of ρ are now shown with respect to Scenarios #1 and #2. At 35 dBm launch power, which appears reasonable when considering that such power is spread out over 200 nm of optical bandwidth, a NANF with 0.295 dB/km loss would allow reaching a 2x throughput increase over SMF, at a contained $\mathrm{Ch}_{\mathrm{b/s}}^{\mathrm{NANF}}$ of 8.3 bits/symb. This shows that in this scenario, a quite sizeable throughput increase is attainable in NANF even at a loss significantly higher than SMF. Note that, as it could be surmised, when increasing NANF bandwidth, the problem of prohibitively high $\mathrm{Ch}_{\mathrm{b/s}}$ is substantially alleviated.

If same loss as SMF was achieved (0.2 dB/km), a 3x throughput multiple would be possible at a total launch power of 32.2 dBm and a large but still conceivably manageable $\mathrm{Ch}_{\mathrm{b/s}}^{\mathrm{NANF}}$ of 12.4 bits/symb. Even higher multiples are displayed in Fig. 3, but they should be considered as longer-term prospects, since they require either very large launch power, very low NANF loss or very high $\mathrm{Ch}_{\mathrm{b/s}}^{\mathrm{NANF}}$.

D. Scenario #3 with IMI

The previous results assumed no IMI. To introduce it, Eq. (7) can be used. Fig. 3b shows ρ for Scenario #3 at an IMI of -50 dB/km, similar to what was measured in the recent record experiment [14]. The impact of IMI is clearly visible, with all isolines equal or higher than a multiple 3 disappearing from the plot. Yet, we point out that the 2x isoline is affected relatively little, while the 3x isoline gets essentially replaced by a 2.5x isoline. This shows that the degradation, although clearly present, is relatively modest if the lower multiples of throughput are considered.

To appreciate what value would make IMI essentially irrelevant, in Fig. 3c we show ρ at an IMI of -60 dB/km. Only the highest isolines are affected which, however, correspond to operating points that are probably unrealistic even in the long run. From a practical viewpoint, therefore, the value -60 dB/km is low enough to cause little or no practical impact.

E. Scenario #4: 1500-1700 nm, 3000 km link

This scenario assumes the exact same parameters as Scenario #3, with the only difference of link length being now 3000 km (30 spans of 100 km each) rather than 1000 km.

The results are shown in Fig. 4. The plot is quite similar to Fig. 3a, but in general a slight improvement of ρ can be observed. For instance, at loss 0.2 dB/km and 35 dBm launch power, NANF now delivers 3.8x, whereas over 1000 km it delivered 3.5x.

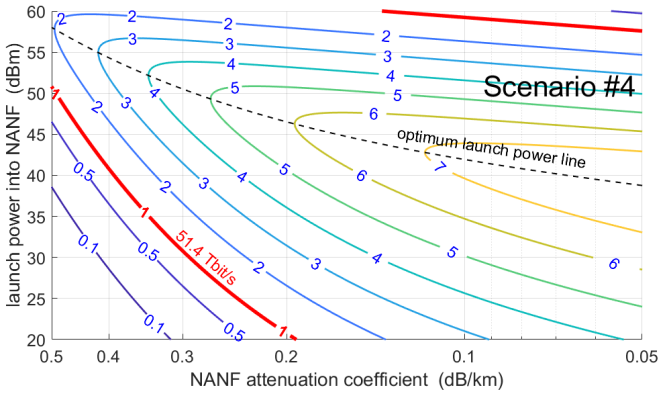

Fig. 4. Scenario #4. Isolines showing the ratio ρ of NANF system throughput vs. the SMF maximum system throughput (51.4 Tb/s), over the plane (NANF loss, NANF launch power). The test link consists of 3000 km of fiber (30 spans of 100 km). The NANF systems operate over the 1500-1700 nm band (23.5 THz), the benchmark SMF system over the C+L bands (9 THz). The red isoline marks the ratio 1, i.e., same NANF throughput as maximum SMF throughput. IMI is assumed absent or negligible.

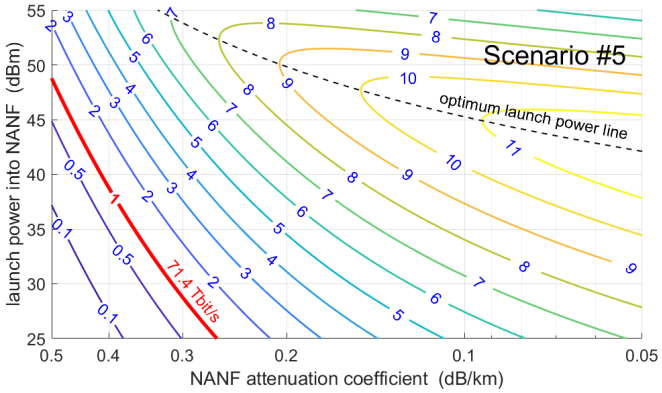

Fig. 5. Scenario #5. Isolines showing the ratio ρ of NANF system throughput vs. the SMF maximum system throughput (71.4 Tb/s), over the plane (NANF loss, NANF launch power). The test link consists of 1000 km of fiber (10 spans of 100 km). The NANF systems operate over the 1450-1850 nm band (44.7 THz), the benchmark SMF system over the C+L bands (9 THz). The red isoline marks the ratio 1, i.e., same NANF throughput as maximum SMF throughput. IMI is assumed absent or negligible.

More significantly, from a practical viewpoint, the multiple 3.5x is obtained at $\mathrm{Ch}_{\mathrm{b/s}}$=14.5 bits/symb in Scenario #3, over 1000 km, whereas in Scenario #4, over 3000 km, the multiple 3.5x is found at $\mathrm{Ch}_{\mathrm{b/s}}$=10.4 bits/symb. While the former value of $\mathrm{Ch}_{\mathrm{b/s}}$ is problematic, the latter is large but attainable. This shows again that, as expected, the problem of high $\mathrm{Ch}_{\mathrm{b/s}}$ gets progressively alleviated when operating over longer distances.

Like we did for Scenario #3, we re-ran the calculations with non-zero IMI for Scenario #4. The degradation is qualitatively and quantitatively very similar to what is seen in Scenario #3 (figures are omitted for brevity). Here too, when IMI goes below -60 dB/km it has little practical impact, as it only substantially affects multiples from 4x and upward.

F. Scenario #5: 1450-1850 nm, 1000 km link

The previous scenarios have shown a potential throughput increase of 1.5x to 3.5x, when considering values of loss,

launch power and $\mathrm{Ch_{b/s}}$ that are conceivably achievable in the not-too-distant future. These multiples are quite significant, but perhaps only evolutionary, rather than constituting a revolutionary 'quantum leap'.

NANF, however, might be able, at least theoretically, to deliver even better performance than the scenarios shown so far. Low-loss over bandwidths as broad as 400 nm (about 45 THz), or even broader, has been predicted [6], [29]. Assuming this was indeed possible in the future, such ultra-broadband scenario would indeed potentially represent a revolutionary quantum leap.

Fiber would however not be the only critical aspect in such ultra-broadband scenarios: amplification would be as critical. Some proposed technologies appear to be promising in this respect. For example, Bismuth-doped fiber amplifiers have been shown to potentially offer gain over an extremely broad spectral range, at a performance that is not too distant from conventional EDFAs [30], [31]. However, it is almost certain that many amplification units in parallel, each one devoted to a specific sub-band, would be needed to cover multi-hundred-nm bandwidths. This causes a possible scaling penalty that has rightly been pointed out in the literature [1].

Therefore, while in this section we assume that the problem of ultra-broadband amplification has been acceptably dealt with, in the next section we will provide an alternative path to the exploitation of the ultra-broadband features of NANF that either drastically reduces the number of needed amplifiers or completely removes them from the system.

Even assuming that ultra-broadband amplifiers were available, it is likely that the average noise figure might be degraded and, to be conservative, we assume here NF= 9 dB. Our reference comparison case remains SMF over C+L, with NF= 0 dB (thanks to Raman). Fig. 5 then shows the results of ρ for this scenario, over 1000 km (10 spans of 100 km each).

A 3x throughput increase is possible even at a higher-than-SMF loss of 0.28 dB/km and launch power 35 dBm, with $\mathrm{Ch}_{\mathrm{b/s}}^{\mathrm{NANF}}$ being a comfortable 6.6 bits/symb. If NANF loss arrived on a par with SMF, again at 35 dBm launch power a 5x would be possible at a still manageable $\mathrm{Ch}_{\mathrm{b/s}}^{\mathrm{NANF}}$ = 10.9 bits/symb. Also, 6x would not be out of the question, requiring higher power (but spread out over an extremely large optical bandwidth) and a challenging but perhaps not impossible $\mathrm{Ch}_{\mathrm{b/s}}^{\mathrm{NANF}}$ = 13.1 bits/symb.

We further tested Scenario #5 by extending it to 3000 km. The throughput ratio plot changes relatively little vs. Fig. 5, but the needed $\mathrm{Ch_{b/s}}$ shrinks quite notably for any given multiple. Specifically, the 5x multiple is found at the same launch power (35 dBm) and same loss (0.2 dB/km) as over 1000 km, but the value of $\mathrm{Ch_{b/s}}$ goes down from 10.9 bits/symb to 7.85 bits/symb, substantially easing its possible achievement. This is a significant result from a practical viewpoint.

We also added IMI. A very similar behavior was found to when we introduced IMI in previous scenarios. We do not show the figures for brevity. Essentially, once again a value of less than -60 dB/km makes IMI practically irrelevant.

V. Repeaterless and Amplifierless Scenarios

As mentioned earlier, large available bandwidth in fiber does not automatically grant equally enhanced throughput, since suitable amplification is needed to support such extended bandwidth.

However, besides offering ultra-broad bandwidth, NANF (and possibly evolutions thereof) holds the promise for ultra-low loss, even lower than SMF. In this section we assume that such lower-than-SMF loss is reachable in the future and exploit it to explore two further scenarios in which amplifiers are either removed from the line (repeaterless, Scenario #6) or removed altogether from the system (Scenario #7). The important caveat here is that we are speculating on possible technological evolution that, though not barred by theory at present, might or might not prove feasible.

Also, we limit the reach to 250-300 km. While this distance is much less than the previous scenarios, it is still a practically significant distance for core networking in many densely populated areas, like most of Europe, Japan, areas of the East and West coast of the US, areas of China, as well as many others.

With this in mind, we first look at the *repeaterless scenario*.

A. Scenario #6: 1450-1850 nm, 250-300 km repeaterless link

The attractiveness of such a scenario is the ideal possibility of making the potentially ultra-wide band of NANFs more easily exploitable. Doing away with line amplifiers would greatly simplify the transmission line, which becomes 'single-span', and simplify the overall system as a consequence. The scalability problem involved in the need to amplify the full band of each NANF, possibly with multiple parallel sub-band units, at each repeater site, is hence avoided.

In this scenario we still assume that amplifiers are available at the receiver site, with an average NF of 7 dB. We also keep assuming, as done so far, that the receivers have an additional back-to-back penalty of 3 dB in all configurations.

We first set the link length to 250 km, single-span. We then conjecture that NANFs are capable of achieving a loss between 0.13 and 0.05 dB/km. We also suppose that such loss is available over a bandwidth spanning the full 1450-1850 nm range (44.7 THz). In such ultra-low-loss context, splice loss cannot be neglected. We therefore assume that in the cable there is a splice every 5 km, at an average splice loss of 0.1 dB, totaling a fixed 5 dB of extra loss over the link length.

Fig. 6 shows the results. They are no longer displayed as a ratio of NANF throughput vs. SMF throughput, since in this context a direct comparison with SMF largely loses meaning. Instead, the NANF absolute throughput T_{NANF} in Tb/s is shown. At a relatively contained 35 dBm launch power and at 0.1 dB/km loss, a quite significant throughput of 400 Tb/s (per fiber) is ideally achievable, at $\mathrm{Ch_{b/s}}$=12.22 bits/symb.

If we then increase the distance to 300 km, at the same loss and launch power, almost 300 Tb/s per fiber are achieved, at $\mathrm{Ch_{b/s}}$= 9.2 bits/symb (not shown for brevity). Finally, adding IMI at -60 dB/km has essentially no effect on the above-discussed operating points, impacting only higher-multiple but less realistically achievable operating points.

This article has been accepted for publication in IEEE/OSA Journal of Lightwave Technology. This is the author's version which has not been fully edited and content may change prior to final publication. Citation information: DOI 10.1109/JLT.2021.3140114

B. Scenario #7: 1450-1850 nm, 250-300 km amplifierless link with high-LO-power receivers

In the previous scenario we assumed that optical amplifiers were still present at the start/end nodes of the link. In Scenario #7 we explore the possibility of completely removing optical amplifiers from the system.

We still assume that NANF operates over the 1450-1850 nm band, as in the previous scenario. We point out that the amplifierless context could potentially usher access to even larger bandwidths, which ideally NANFs seems to be capable of supporting [11]. We will however not address broader bandwidth values in this paper.

A specific challenge of this completely amplifierless context is that the receiver does not use a front-end optical pre-amplifier to boost the signal. Interestingly, the ideally achievable performance of a coherent receiver that has no optical pre-amplifier is the same as that of an optically pre-amplified receiver. The corresponding ideal maximum SNR, given a received power $P_{\mathrm{ch}}^{\mathrm{Rx}}$ at the input of the receiver, is in both cases [32]–[34]:

$$\mathrm{SNR}_{\mathrm{ideal}} = \frac{P_{\mathrm{ch}}^{\mathrm{Rx}}}{2\,h\nu\,R_{\mathrm{ch}}} \tag{11}$$

For receivers without optical pre-amplifier this limit is achieved assuming[1]:

- ideal photodetector responsivity, i.e., equal to $q/h\nu$ A/W, where q is the electron charge
- arbitrarily large local-oscillator (LO) power (large enough to make electrical receiver noise negligible)
- perfectly symmetric optical hybrid front-end and perfectly balanced photodetectors, resulting in complete suppression of LO relative intensity noise (RIN); alternatively, negligible LO RIN
- no excess loss between receiver input and photodetectors.

In practice, none of the above conditions is exactly met. This means that *a SNR penalty is always incurred* vs. the value of Eq. (11). However, a recent paper has shown that a standard commercial receiver, not specifically optimized for operation without optical pre-amplifier, when supplied with a high-power (14 dBm) LO, achieved a sensitivity which was, remarkably, only 5.5 dB away from Eq. (11). The result was found using 28 GBaud PM-QPSK modulation. It also achieved a sensitivity 7.5 dB away from Eq. (11), with 28 GBaud PM-16QAM modulation [35]. Both results refer to pre-FEC BER= 10^{-2}.

In this work we are certainly targeting higher Baud rates and higher bits/symb than in [35] and this would suggest that a higher penalty than found in [35] could be incurred. On the other hand, we surmise that specific design and manufacturing optimization for LO-only receivers could be carried out in the future, which is not currently done for receivers that are meant to operate with optical pre-amplifiers. Taking these different aspects into account, it appears to us that a reasonably conservative hypothesis is to assume a penalty of 10 dB with respect to the ideal limit of Eq. (11).

[1]For comparison, for conventional receivers using an optical pre-amplifier the same limit Eq. (11) is achieved assuming: arbitrarily high optical pre-amplifier gain (high enough to make electrical receiver noise negligible), no LO RIN or equivalently no asymmetry in either the optical hybrid front-end or balanced photodetectors, no excess loss between receiver input and photodetectors.

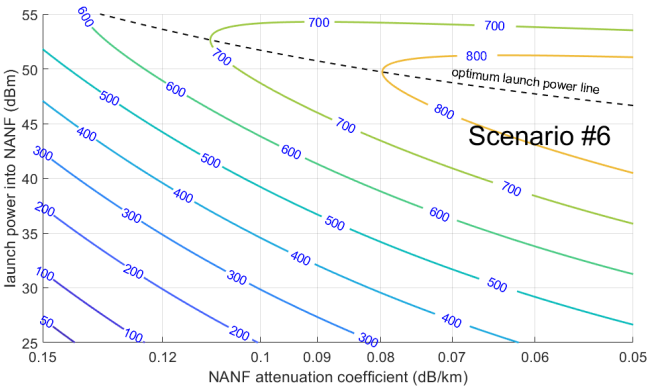

Fig. 6. Scenario #6. NANF system throughput isolines (Tb/s) over the plane (NANF loss, NANF launch power). The NANF systems operate over the 1450-1850 nm band (44.7 THz). Repeaterless single-span of 250 km. IMI is assumed absent or negligible.

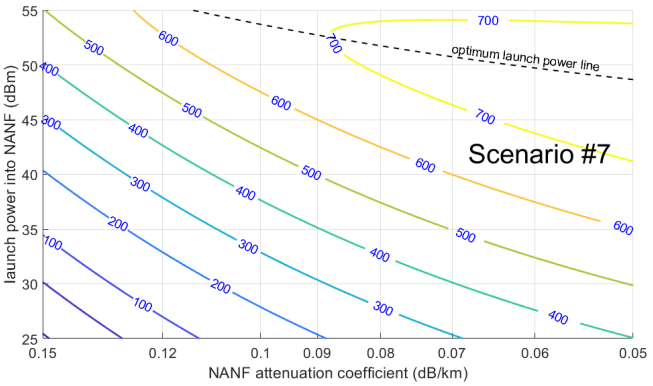

Fig. 7. Scenario #7. NANF system throughput isolines (Tb/s) over the plane (NANF loss, NANF launch power). The NANF systems operate over the 1450-1850 nm band (44.7 THz). Amplifierless single-span of 250 km. IMI is assumed absent or negligible. The receivers are assumed to operate with a 10 dB SNR penalty vs. the ideal value of Eq. (11).

With this assumption, the results of NANF system throughput for a 250 km single-span link are shown in Fig. 7. They are somewhat less favorable than for Scenario #6 but still about 330 Tb/s of throughput is delivered at 35 dBm launch power and loss 0.1 dB. Notice also that the values are very sensitive to NANF loss. A 1/100 dB/km decrease in loss would boost throughput up to 400 Tb/s.

Of course these completely amplifierless links would easily be impacted by any excess loss. On the other hand, such loss could be compensated for by raising launch power by an equal amount. Since NANF exhibits ultra-low non-linearity raising launch power is possible ideally up to very high values, the limit being induced by considerations other than system performance (such as for instance safety). Loss can also be managed by accepting a reduction in throughput, by about 1 bit/symb every 3 dB of extra loss. Margins are therefore present that could be tapped into.

This article has been accepted for publication in IEEE/OSA Journal of Lightwave Technology. This is the author's version which has not been fully edited and content may change prior to final publication. Citation information: DOI 10.1109/JLT.2021.3140114

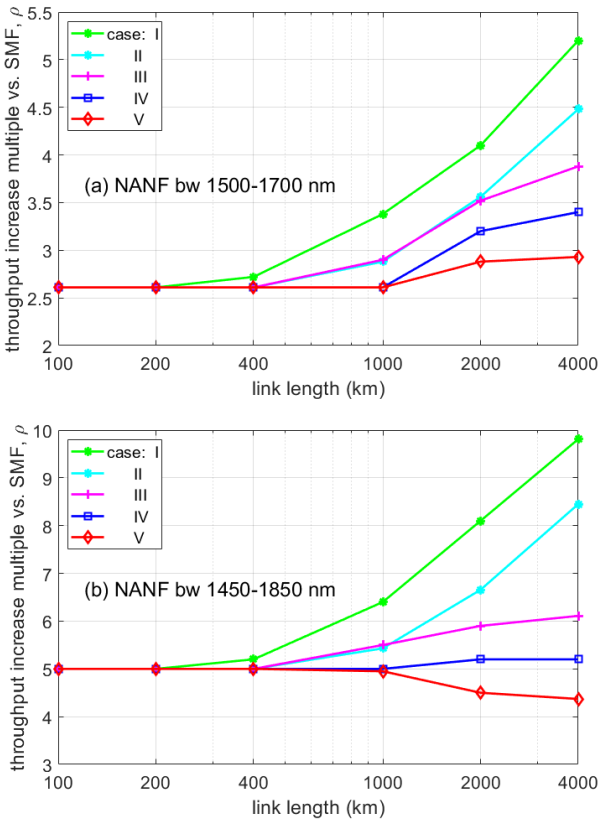

Fig. 8. Ratio ρ of NANF system throughput vs. SMF maximum system throughput as a function of link length. Span length is 100 km. The benchmark SMF system operates over the C+L bands (9 THz) with Raman amplification (effective noise figure 0 dB). The different curves use the further assumptions shown in Table I. NANF system optical bandwidth: **(a)** 1500-1700 nm (23.5 THz); **(b)** 1450-1850 nm (44.7 THz). NANF system amplifier noise figure: 9 dB in all cases.

TABLE I
ASSUMPTIONS USED TO DRAW FIG. 8.

case	NANF loss dB/km	max launch power into NANF, dBm	max tx/rx SE bits/symb
I	0.15	40	14
II	0.15	40	12
III	0.2	37	12
IV	0.2	35	11
V	0.2	33	10

VI. DISCUSSION OF EMERGING LANDSCAPE

As we have shown for the several scenarios that we have presented, the concomitance of ultra-low non-linearity, low loss and large bandwidth creates the potential for building NANF systems capable of delivering significant multiples of the throughput of the benchmark system based on the current SMF 'sweet-spot' consisting of C+L+Raman.

While the maps that we have shown provide a very detailed picture of each specific scenario, in this section we try to provide a more general view of the overall 'landscape', across a wide range of system lengths. To do so, we first set certain general constraints which we impose on three key elements: the maximum transponder spectral efficiency (SE, in bits/symb); the maximum acceptable launch power; a specific value of NANF loss. We put together 5 combinations of their values, which are shown in Table I. Case V is the most conservative, in the sense that we assume SE values and launch powers that are achieved even in current SMF commercial systems using Raman amplification. Also, NANF loss is assumed to be on a par with SMF. Cases IV to I are increasingly less conservative, but we believe none is unrealistic, at least in the long run. Note that when we impose a certain limitation on the SE of the NANF system transponders, we of course impose *the same* limitation on the SMF system transponders, too.

The throughput multiples corresponding to the different cases are shown in Fig. 8, as a function of system length. In (a) we assume a NANF bandwidth of 23.5 THz (1500-1700 nm) and in (b) of 44.7 THz (1450-1850 nm). In both these plots, the amplifiers for the NANF systems are conservatively considered to have 9 dB noise figure, vs. 0 dB *effective* noise figure for SMF (thanks to Raman amplification). Note that span length is kept constant at 100 km, which is a reasonable assumption for terrestrial systems.

Fig. 8 shows that, for short distances, all cases converge towards one value, which is about $\rho = 2.6$ for the 23.5 THz systems and $\rho = 5$ for the 43.7 THz systems. These values simply represent the ratio between the assumed NANF bandwidth and the assumed SMF C+L bandwidth (9 THz). What happens is that the maximum allowed transponder SE is achieved while still well within the linear regime for SMF and well below the max launch power for NANF. As a result the respective transmission links become 'transparent' for both fibers and the throughput multiple achieved by NANF is simply the raw optical bandwidth ratio of NANF vs. SMF. Note that even though NANF operates at a large noise-figure disadvantage vs. SMF (9 dB gap), this is compensated for by launching a higher power into NANF.

Moving towards longer distances, then we see a quick increase of multiples for case I (green curve). This happens because the SMF reaches its non-linear limit and its system throughput starts going down. NANF instead can maintain throughput by increasing launch power, which case I allows to raise up to 40 dBm. NANF ultra-low non-linearity ensures that this can be done with no significant signal degradation.

All other cases grow less than case I, because they either hit their launch power limit or their SE constraint. As a general rule, the SE limitation is typically hit for low-to-intermediate distances (up to about 1,000 km). Moving to longer distances, it is the maximum launch power constraint that intervenes.

Whichever the limiting constraint, all curves grow, with only one exception: Fig. 8(b), case V (red curve). Analyzing that system at 2000km, it is found that it is the launch power constraint of 33 dBm that causes this behavior. Specifically, the launch power required to go back up to the multiple $\rho = 5$ would be a higher 34.5 dBm. The SE limit plays no role here, since it would be reached at 36.4 dBm launch power.

Fig. 8 provides, in our view, a quite encompassing picture of what can be expected in the NANF-SMF comparison. As a rather general emerging feature, a throughput multiple at least equal to the optical bandwidth ratio should be achievable. Even greater multiples might be reached, especially if significant

amounts of power can be launched into the NANF.

These results appear to show that NANF might establish a new paradigm in potential system throughput. Its very wide bandwidth is possibly its most important asset, with ultra-low non-linearity being a close runner-up.

Note that outstanding landmark papers such as [37] seem to be at odds with our results since they showed that reducing fiber non-linearity, even substantially, would bring about only a marginal increase in throughput. Same was shown for loss. Our findings are not in disagreement with those results. The new factor here is that NANF combines a dramatic reduction in non-linearity (and possibly a reduction in loss as well) with a much increased usable bandwidth. It is the combination of these features that turns out to be very effective in increasing potential throughput.

As already mentioned in Sect. IV-F, the availability of a very broad bandwidth does not guarantee that its exploitation is easy. This was already remarked in [37] and has been further pointed out in [1] and other literature. In particular, broadband amplification is a challenge and would probably require sub-band specific units in parallel. On the other hand, optical and optoelectronic technology have made giant leaps over and again, and the availability of fibers with potentially 5x greater throughput than current ones might in the end spur the development of effective supporting technologies, that at present are difficult to predict.

As either an alternative, or a synergistic possibility, NANF might make it possible to perform repeaterless or amplifierless transmission, as analyzed in Sect. V. Regarding these scenarios, in some respects their discussion is more straightforward and in some other it is more complex than optically amplified scenarios. The plots tell us that, provided NANF loss goes down to 0.1 dB/km, then it would be possible to transmit half a Pbit/s per NANF over regional distances of 200-300 km (see Figs. 6–7). If this was the case, the impact on network architecture could be far-reaching, though hard to predict. We consider the topic of architecture more on the side of networking and outside of the scope of this paper, so we refrain from discussing it here.

VII. Conclusion

Hollow-core fibers of the nested anti-resonant nodeless type (NANFs) have recently entered the realm of those competing technologies that are being developed to overcome the throughput limitations of the traditional single-core, single-mode, silica-core fiber.

By analytical means, validated through simulations, we have shown that NANFs could potentially provide a total throughput that ranges between 1.5 and 5-6 times that of a benchmark system consisting of SMF with Raman amplification over the C+L bands. These results are obtained at NANF loss levels equal or even slightly higher than SMF. When considering the evolution of reported NANF loss over the last few years, such loss levels appear to be attainable in the not-too-distant future.

If even lower loss, which could theoretically be possible, proved practically achievable, the scenario of repeaterless or amplifierless ultra-broad-band transmission over NANF would open up. Assuming 0.1 dB/km loss, half a Petabit/s per fiber could be achieved over 200-300 km, with a potentially large and not just evolutionary impact on optical data transport networks performance and architecture.

Besides loss, IMI must also be kept in check. We have shown consistently that a value of -60 dB/km would be sufficient to make it practically negligible. Since the current best NANF specimens approach or achieve this value, this effect appears to be on a path towards being reigned in.

It must be acknowledged that, to make the above scenarios realistic, substantial challenges need to be addressed, not just related to NANF performance. Among them, unconventional band amplification technologies for repeatered systems, transponders supporting transmission at high net bits/symbol per channel, management of large launched powers. In prospect, for repeaterless and amplifierless systems, also the optimization of receiver design and manufacturing for LO-only (no optical pre-amplifier) operation and the minimization of all types of excess loss, such as from splicing, cabling and mux/demux components.

Optical technology progress has however achieved surprising breakthroughs time and again, over its relatively short history, and we believe that there is a possibility that NANF and NANF-based systems could be one of these breakthroughs.

References

[1] P. Winzer, D. Neilson, A. Chraplyvy ‘Fiber-optic transmission and networking: the previous 20 and the next 20 years,’ *Optics Express*, vol. 26, no. 18, pp. 24190–24239, Sept. 2018.

[2] P. Sillard, M. Bigot-Astruc and D. Molin, ‘Few-mode fibers for mode-division-multiplexed systems,’ *J. of Lightwave Technol.*, vol 32, no. 16, pp. 2824-2829, Aug. 2014.

[3] Kunimasa Saitoh and Shoichiro Matsuo, ‘Multicore Fiber Technology,’ *J. of Lightwave Technol.*, vol. 34, no. 1, pp. 55-66, Jan. 2016.

[4] A. Ferrari, E. Virgillito, V. Curri, ‘Band-Division vs. Space-Division Multiplexing: A Network Performance Statistical Assessment,’ *J. of Lightwave Technol.*, vol. 38, no. 5, pp. 1041–1049, Mar. 2020.

[5] R. F. Cregan, B. J. Mangan, J. C. Knight, T. A. Birks, P. St.J. Russell, P. J. Roberts, and D. C. Allan, ‘Single-mode photonic band gap guidance of light in air,’ *Science*, 285, 1537–1539, 1999.

[6] F. Poletti, ‘Nested antiresonant nodeless hollow core fiber,’ *Opt. Express*, vol. 22, pp. 23807–23828, 2014.

[7] A. D. Pryamikov et al., ‘Demonstration of a waveguide regime for a silica hollow-core microstructured optical fiber with a negative curvature of the core boundary in the spectral range > 3.5 μm,’ *Opt. Express*, 19, pp. 1441-1448 (2011).

[8] W. Belardi and J. C. Knight, ‘Hollow antiresonant fibers with reduced attenuation,’ *Opt. Lett.*, 39(7), pp. 1853-1856 (2014).

[9] T.D. Bradley, J.R. Hayes, Y. Chen, G. T. Jasion, S. R. Sandoghchi, R. Slavik, E. N. Fokoua, S. Bawn, H. Sakr, I.A. Davidson, , A. Taranta, J. P. Thomas, M. N. Petrovich, D.J. Richardson and F. Poletti: ‘Record Low-Loss 1.3dB/km Data Transmitting Antiresonant Hollow Core Fibre,’ in *Proc. ECOC 2018*, Rome, Italy, paper PDP Th3F.2.

[10] T. D. Bradley, G. T. Jasion, J. R. Hayes, Yong Chen, L. Hooper, H. Sakr, M. Alonso, A. Taranta, A. Saljoghei, H. C. Mulvad, M. Fake, I. A. Davidson, N. V. Wheeler, E. N. Fokoua, Wei Wang, S. Reza Sandoghchi, D. J. Richardson, F. Poletti, ‘Antiresonant Hollow Core Fibre with 0.65 dB/km Attenuation across the C and L Telecommunication Bands,’ in *Proc. ECOC 2019*, post-deadline paper PD3.1, Dublin (IL), Sept. 2019.

[11] G. T. Jasion, T. D. Bradley, K. Harrington, H. Sakr, Yong Chen, E. Numkam Fokoua1, I. A. Davidson, A. Taranta, J. R. Hayes, D. J. Richardson, F. Poletti ‘Hollow Core NANF with 0.28 dB/km Attenuation in the C and L Bands,’ *in Proc. OFC 2020*, post-deadline paper Th4B.4, San Diego (CA), March 2020.

[12] A. Nespola et al, ‘Record PM-16QAM and PM-QPSK Transmission Distance (125 and 340 km) over Hollow-Core-Fiber,’ *in Proc. ECOC 2019*, paper PD.1.5, Dublin (IE), Sept. 2019.

[13] A. Nespola et al, 'Transmission of 61 C-Band Channels Over Record Distance of Hollow-Core-Fiber With L-Band Interferers,' *J. of Lightw. Technol.*, vol. 39, no. 3, pp. 813-820, Feb. 2021.

[14] A. Nespola et al, 'Ultra-Long-Haul WDM Transmission in a Reduced Inter-Modal Interference NANF Hollow-Core Fiber,' *in Proc. OFC 2021*, post-deadline paper F3B.5, San Francisco (USA), June 2021.

[15] P. Poggiolini, F. Poletti, 'Opportunities and Challenges for Long-Distance Transmission in Hollow-Core Fibres,' *in Proc. OFC 2020*, paper F4C.1, San Francisco (USA), June 2021.

[16] E. A. J. Marcatili and R. A. Schmeltzer, 'Hollow Metallic and Dielectric Waveguides for Long Distance Optical Transmission and Lasers,' *Bell Syst. Tech. J.*, vol. 43, no. 4, pp. 1783-1809, 1964.

[17] F. Poletti, M. Petrovich, M. and D. J. Richardson, 'Hollow-core photonic bandgap fibers: technology and applications,' *Nanophotonics*, vol. 2, issue 5-6, pp. 315-340, 2013.

[18] V. Michaud-Belleau et al., 'Backscattering in antiresonant hollow-core fibers: over 40 dB lower than in standard optical fibers,' *Optica*, vol. 8, no. 2, p. 216, Feb. 2021.

[19] N. Takefushi, M. Yoshida, K. Kasai, T. Hirooka, and M. Nakazawa, 'Theoretical and experimental analyses of GAWBS phase noise in various optical fibers for digital coherent transmission,' *Optics Express*, vol. 28, no. 3, p. 2873, 2020.

[20] I. A. Bufetov, A. N. Kolyadin, A. F. Kosolapov, V. P. Efremov, V. E. Fortov, 'Catastrophic damage in hollow core optical fibers under high power laser radiation,' *Optics Express*, vol. 27, no. 13, pp. 18296-18310, 2019.

[21] M. Ohashi, K. Shiraki and K. Tajima, 'Optical loss property of silica-based single-mode fibers,' *J. of Lightwave Technol.*, vol. 10, no. 5, pp. 539-543, May 1992.

[22] Y. Tamura et al., 'The First 0.14-dB/km Loss Optical Fiber and its Impact on Submarine Transmission,' *J. of Lightwave Technol.*, vol. 36, no. 1, pp. 44-49, 1 Jan.1, 2018.

[23] D. Suslov, M. Komanec, E. R. Numkam Fokoua, D. Dousek, A. Zhong, S. Zvnovec, T. D. Bradley, F. Poletti, D. J. Richardson, R. Slavk, 'Low loss and high performance interconnection between standard single-mode fiber and antiresonant hollow-core fiber,' *Nature Scientific Reports*, **11**, 8799 (2021).

[24] G. Bosco, P. Poggiolini, A. Carena, V. Curri, F. Forghieri, 'Analytical Results on Channel Capacity in Uncompensated Optical Links with Coherent Detection,' *Opt. Express*, vol. 19, no. 26, pp. B438–B49, 2011. See also, by the same authors: '- Erratum' (corrections), *Opt. Express*, vol. 20, no. 17, pp. 19610–19611, 2012.

[25] J. M. Gen, P. J. Winzer, 'A Universal Specification for Multicore Fiber Crosstalk,' *IEEE Phot. Tech. Lett.*, vol. 31, no. 9, pp. 673–676, May 2019.

[26] P. Poggiolini, 'The GN model of non-linear propagation in uncompensated coherent optical systems,' *J. of Lightwave Technol.*, vol. 30, no. 24, pp. 3857-3879, Dec. 2012.

[27] A. Nespola, S. Straullu, A. Carena, G. Bosco, R. Cigliutti, V. Curri, P. Poggiolini, M. Hirano, Y. Yamamoto, T. Sasaki, J. Bauwelinck, K. Verheyen, and F. Forghieri, 'GN-model validation over seven fiber types in uncompensated PM-16QAM Nyquist-WDM links,' IEEE Photonics Technology Letters, vol. 26, no. 2, pp. 206-209, Jan. 2014.

[28] P. Poggiolini, Y. Jiang 'Recent Advances in the Modeling of the Impact of Nonlinear Fiber Propagation Effects on Uncompensated Coherent Transmission Systems,' Tutorial Review, *J. of Lightwave Technol.*, vol. 35, no. 3, pp. 458-480, Feb. 2017.

[29] H. Sakr, T.D. Bradley, Y. Hong, G. T. Jasion, J. R. Hayes, H. Kim, I. A. Davidson, E. Numkam Fokoua, Y. Chen, K. R. H. Bottrill, N. Taengnoi, P. Petropoulos, D. J. Richardson, and F. Poletti.: 'Ultrawide Bandwidth Hollow Core Fiber for Interband Short Reach Data Transmission', *Proc. OFC 2019*, paper PDP Th4A.1.

[30] E. Dianov, 'Bismuth-doped optical fibers: a challenging active medium for near-IR lasers and optical amplifiers,' *Light: Science & Applications*, Vol. 1, pp. 1-7, 2012.

[31] Sergei Firstov, Sergey Alyshev, Mikhail Melkumov, Konstantin Riumkin, Alexey Shubin, and Evgeny Dianov, 'Bismuth-doped optical fibers and fiber lasers for a spectral region of 1600-1800 nm,' *Opt. Lett.*, vol. 39, pp. 6927-6930, 2014.

[32] L. Kazovsky, S. Benedetto, A. Willner, *Optical Fiber Communication Systems*, Artech House, Boston, 1996, ISBN: 0-89006-756-2, ISBN 13: 978-0-89006-756-7

[33] Bo Zhang, C. Malouin, T. J. Schmidt 'Design of coherent receiver optical front end for unamplified applications,' *Optics Express*, vol. 20, no. 3, pp. 3225–3234, Jan. 2012.

[34] Kazuro Kikuchi 'Fundamentals of Coherent Optical Fiber Communications,' *J. of Lightwave Technol.*, vol. 34, no. 1, pp. 157–179, Jan. 2016.

[35] G. Rizzelli, A. Nespola, S. Straullu, F. Forghieri, R. Gaudino, 'Scaling Laws for Unamplified Coherent Transmission in Next-generation Short-Reach and Access Networks,' *J. of Lightwave Technol.*, early access, doi: 10.1109/JLT.2021.3092523, 2021.

[36] P. Poggiolini, G. Bosco, A. Carena, V. Curri, Y. Jiang, F. Forghieri, 'The GN model of fiber non-linear propagation and its applications,' *J. of Lightwave Technol.*, vol. 32, no. 4, pp. 694–721, Feb. 2014.

[37] R.-J. Essiambre, R. W. Tkach, 'Capacity Trends and Limits of Optical Communication Networks,' *Proc. IEEE*, vol. 100, no. 5, pp. 1035-1055 (2012).

Pierluigi Poggiolini received his M.S. degree cum laude in 1988 and his Ph.D. degree in 1993 from Politecnico di Torino, Italy. From 1988 to 1989 he was with the Italian State Telephone Company research center CSELT. From 1990 to 1995 he was a Visiting Scholar and then a Post-Doctoral Fellow at the Optical Communications Research Laboratory of Stanford University. Since 2010 he has been a Full Professor at Politecnico di Torino. He was an elected member of the Academic Senate (2005-2010) and of the Board of Directors (2016-2020) of Politecnico di Torino. He was Technical Co-Chair of the ECOC conference in 2010. He has published over 250 papers in leading journals and conferences. He is a co-author of two papers, published in 2011 and 2012, that have received the Journal of Lightwave Technology Best Paper Award. He is an OPTICA and IEEE Fellow. His current research interests include long-haul coherent transmission systems, non-linear fiber effects, modeling and simulation of optical communications systems, hollow-core fiber transmission systems.

Francesco Poletti (Member, IEEE) received the Laurea degree in electronics engineering from the University of Parma, Parma, Italy, in 2000, and the Ph.D. degree from the Optoelectronics Research Centre (ORC), University of Southampton, Southampton, U.K., in 2007. He is currently a Professor with ORC. He has worked for three years on optical network design with Marconi Communications and for more than ten years on the development of new generations of microstructured optical fibers with the ORC. He has coauthored more than 80 journal and 200 conference publications, and produced four patents. His research interests include the design of photonic bandgap and antiresonant fibers, the development of fiber-optic characterization techniques, and the fabrication of nonsilica-based fibers and devices. He is the holder of a European Research Fellowship Consolidator Grant.